C. R. Mecanique 339 (2011) 12–19

Contents lists available at ScienceDirect

Comptes Rendus Mecanique

www.sciencedirect.com

Periodic boundary conditions for the numerical homogenization of composite tubes

Conditions aux limites périodiques pour l'homogénéisation numérique de tubes composites

Lionel Gélébart

CEA-Saclay, DEN/DMN/SRMA, 91190 Gif-sur-Yvette, France

ARTICLE INFO

Article history:
Received 25 October 2010
Accepted after revision 23 December 2010
Available online 11 January 2011

Keywords:
Solids and structures
Tube
Composites
Boundary conditions
Homogenization
Elasticity

Mots-clés :
Solides et structures
Tube
Composites
Conditions aux limites
Homogénéisation
Élasticité

ABSTRACT

In order to evaluate the stress-strain fields within periodic composites, finite element simulations are commonly performed on representative unit-cells. For flat composites, periodic boundary conditions are well established and widely used. In the present paper, the definition of periodic boundary conditions is extended to non-flat unit-cells in order to account for the radius of the tube in the simulation. Two different homogenization procedures, based on the simulations performed with these new boundary conditions, are then proposed in order to discuss the validity, as a function of the tube diameter, of a flat unit-cell approximation.

RÉSUMÉ

Afin d'évaluer les contraintes et déformations au sein de matériaux composites périodiques, des simulations par élément-finis sont réalisées sur des cellules représentatives. Pour des composites « plans », les conditions aux limites périodiques sont bien établies et largement utilisées. L'objet de cette note est de détailler les conditions aux limites périodiques à appliquer dans le cas d'une cellule non « plane ». Deux procédures d'homogénéisation prenant en compte les simulations réalisées avec ce nouveau jeu de conditions aux limites sont par la suite proposées dans le but de discuter, en fonction du diamètre du tube, la validité d'une approximation « plane » de la cellule.

1. Introduction

This article focuses on the elastic homogenization of tubes having a coarse microstructure (i.e. the typical length scale of the microstructure is not small compared to the thickness or the radius of the tube). Since taking into account the detailed description of the microstructure would be computation time consuming, rapid and efficient thermo-mechanical simulations require a homogeneous behaviour (i.e. cylindrically distributed). In addition, the microstructure is assumed to be periodic and in the case of the tube, the periodic unit-cell is non-flat. Homogenization of tubes has been treated analytically for thin multi-layered tubes [1,2] and for braided microstructures in the context of the classical plate theory [3]. To the knowledge of the author, the question of the numerical homogenization of tubes based on non-flat periodic unit-cells has not yet been

E-mail address: lionel.gelebart@cea.fr.

1631-0721/$ – see front matter
doi:10.1016/j.crme.2010.12.010

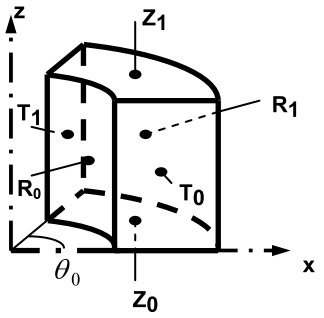

Fig. 1. Description of the non-flat unit-cell.

treated, except by considering flat unit-cells with classical periodic boundary conditions and as a consequence by neglecting the effect of the radius of the tube (see [4], for example). However, the validity of this assumption has to be discussed as a function of the tube diameter. Hence, the main purposes of this paper are, first to define periodic boundary conditions for the tube geometry (i.e. for non-flat unit-cells), and secondly, to propose two different homogenization procedures accounting for these specific boundary conditions in order to discuss the flat unit-cell approximation. These procedures converge towards the flat unit-cell approximation for large enough diameters. Note that for too small diameters, the question itself of replacing the heterogeneous media by homogeneous media has still to be clarified and is out of the scope of this paper. An application is proposed for the case of a tube with spherical inclusions periodically distributed in order to identify the diameter value below which the flat unit-cell approximation is no more relevant.

2. Periodic homogenization for flat unit-cell

The effective behaviour of an infinite and periodic material can be deduced from simulations performed on a periodic unit cell by using classical periodic boundary conditions [5] (Eq. (1), where $\underline{h}$ is a periodicity vector and $\underline{\underline{E}}$ is the applied macroscopic strain). The elastic stiffness tensor can be fully determined from the average stress and strain, evaluated for 6 independent loadings, by solving the 36×36 linear system (Eq. (2), subscript I being associated to each loading). This definition is referred as the "mechanical" approach [6]. Alternatively, the stiffness tensor, can be defined from an "energetic" [6] approach by solving the 36×36 linear system (Eq. (3)).

$$\underline{u}(\underline{x}+\underline{h}) = \underline{u}(\underline{x}) + \underline{\underline{E}}.\underline{h} \tag{1}$$

$$\overline{\underline{\underline{\sigma_I}}} = K_{BC}^{app} : \overline{\underline{\underline{\varepsilon_I}}} \qquad (\text{for } I = 1, \ldots, 6) \tag{2}$$

$$\overline{\underline{\underline{\sigma_I}}} : \underline{\underline{\varepsilon_J}} = \overline{\underline{\underline{\varepsilon_I}}} : K_{BC}^{app} : \overline{\underline{\underline{\varepsilon_J}}} \quad (\text{for } I = 1, \ldots, 6 \text{ and } J = 1, \ldots, 6) \tag{3}$$

As the periodic boundary conditions satisfy the Hill–Mandel condition, these two approaches are equivalent [5] and the resulting stiffness tensor is symmetric.

3. Periodic boundary conditions for non-flat unit-cells

In this section a tube is considered with a periodic microstructure in the axial and circumferential directions. The inner and outer surfaces are subjected to homogeneous stresses. The purpose of this section is to establish the set of periodic boundary conditions to apply on a periodic non-flat unit-cell in order to avoid the simulation of the whole tube. The boundary is divided into 6 surfaces: T_0, T_1, Z_0, Z_1, R_0 and R_1 defined according to Fig. 1. The inner and outer diameters are respectively r_0 and r_1, the angular sector defining the unit-cell is characterized by the angle θ_0. The 6 independent loadings (axial stress, internal pressure, external pressure, axial shear, radial shear and torsion) defined below are related to 6 scalar values (respectively σ_{zz}^0, σ_{rr}^{0i}, σ_{rr}^{0e}, σ_{rz}^{0i}, $\sigma_{r\theta}^{0i}$ and $\mathrm{d}\theta^0$). As they all satisfy the periodicity conditions, any combination (superposition) of them also satisfies the periodicity condition and these 6 independent loadings allow to define a whole set of periodic loadings. The implementation of periodic boundary conditions in a displacement finite-element code (CAST3M in this study) consists of static boundary conditions added to kinematic relations in order to fulfil the periodicity conditions.

3.1. Static boundary conditions

3.1.1. Axial stress σ_{zz}^0

To prescribe axial stresses, the surfaces Z_0 and Z_1 are subjected to uniform axial stresses (Eq. (4)).

$$\underline{\underline{\sigma}}.\underline{e_z} + \underline{r} = -\sigma_{zz}^0 \underline{e_z} \quad \text{on } Z_0 \quad \text{and} \quad \underline{\underline{\sigma}}.\underline{e_z} + \underline{r} = \sigma_{zz}^0 \underline{e_z} \quad \text{on } Z_1 \tag{4}$$

In these equations $\underline{r}$ corresponds to the stress fluctuations induced by the additional kinematic boundary conditions introduced in the following (see Section 3.2.2 and comments in Section 3.3), they are unknown quantities. Practically, the surface forces applied in the finite element code corresponds to the right side of these equations.

3.1.2. Internal and external pressure σ_{rr}^{0i} and σ_{rr}^{0e}

To prescribe internal and external pressures, the surfaces R_0 and R_1 are subjected to uniform radial stresses (Eq. (5)).

$$\underline{\underline{\sigma}}.\underline{e_r} = \sigma_{rr}^{0i}\underline{e_r} \quad \text{on } R_0 \quad \text{and} \quad \underline{\underline{\sigma}}.\underline{e_r} = -\sigma_{rr}^{0e}\underline{e_r} \quad \text{on } R_1 \tag{5}$$

3.1.3. Axial shear σ_{rz}^{0i}

To prescribe axial shears, the surfaces R_0 and R_1 are subjected to uniform axial shear stresses (Eq. (6)).

$$\underline{\underline{\sigma}}.\underline{e_r} = \sigma_{rz}^{0i}\underline{e_z} \quad \text{on } R_0 \quad \text{and} \quad \underline{\underline{\sigma}}.\underline{e_r} = -\frac{r_0}{r_1}\sigma_{rz}^{0i}\underline{e_z} \quad \text{on } R_1 \tag{6}$$

3.1.4. Radial shear $\sigma_{r\theta}^{0i}$

To prescribe internal and external pressure, the surfaces R_0 and R_1 are subjected to uniform axial shear stresses (Eq. (7)).

$$\underline{\underline{\sigma}}.\underline{e_r} = \sigma_{r\theta}^{0i}\underline{e_\theta} \quad \text{on } R_0 \quad \text{and} \quad \underline{\underline{\sigma}}.\underline{e_r} = -\frac{r_0^2}{r_1^2}\sigma_{r\theta}^{0i}\underline{e_\theta} \quad \text{on } R_1 \tag{7}$$

Remark. Note that no prescribed stresses are applied on surfaces T_0 and T_1, stresses on these surfaces will arise from the kinematic periodic boundary conditions prescribed in the next section (see also comments in Section 3.3).

3.2. Kinematic boundary conditions

3.2.1. Surfaces T_0 and T_1

Periodic kinematic boundary conditions on the surfaces T_0 and T_1 can be expressed as follows for each couple of opposite points (M_0, M_1): the position of M_1 in the deformed configuration must correspond to the rotation of the angle θ_0 of M_0 in the deformed configuration (Eq. (8)). Eq. (8) can be expressed in the Cartesian coordinate system (Eqs. (9)) for implementation in the FE code.

$$\underline{M_1} + \underline{u}(M_1) = \underline{\underline{R}}(\theta_0) : \left(\underline{M_0} + \underline{u}(M_0)\right) \tag{8}$$

$$u_x(M_1) - u_x(M_0)\cos\theta_0 + u_y(M_0)\sin\theta_0 = x(M_0)\cos\theta_0 - y(M_0)\sin\theta_0 - x(M_1) \tag{9a}$$

$$u_y(M_1) - u_x(M_0)\sin\theta_0 - u_y(M_0)\cos\theta_0 = x(M_0)\sin\theta_0 + y(M_0)\cos\theta_0 - y(M_1) \tag{9b}$$

$$u_z(M_1) - u_z(M_0) = 0 \tag{9c}$$

3.2.2. Surfaces Z_0 and Z_1

The kinematic boundary conditions on surfaces Z_0 and Z_1 have to fulfil the periodicity conditions and to prescribe the torsion loading (characterized by its angle $\mathrm{d}\theta^0$ between the two surfaces). The boundary conditions have to be divided into conditions in the transverse plane (x, y) and conditions in the axial direction (z) (see Fig. 1). For each couple of opposite points (M_0, M_1): the position of M_1 in the deformed configuration must correspond, in the transverse plane, to the rotation of the angle $\mathrm{d}\theta^0$ of M_0 in the deformed configuration (Eq. (10)). The development of this expression in the Cartesian coordinate system is equivalent to Eqs. (9a) and (9b), replacing θ_0 by $\mathrm{d}\theta^0$.

$$\underline{M_1} + \underline{u}(M_1) = \underline{\underline{R}}\left(\mathrm{d}\theta^0\right) : \left(\underline{M_0} + \underline{u}(M_0)\right) \quad \text{in } (x, y) \text{ plane} \tag{10}$$

In the axial direction, as the axial stress is prescribed the axial strain is unknown and the periodicity condition can be expressed for each couple of opposite points (M_0, M_1) with respect to an arbitrary couple of opposite points (P_0, P_1) (Eq. (11)) [7].

$$u_z(M_0) - u_z(P_0) = u_z(M_1) - u_z(P_1) \tag{11}$$

3.3. Comments

The definition of the kinematic boundary conditions in a finite element code, in our case CAST3M (available online at http://www-cast3m.cea.fr), is often performed by introducing Lagrange multipliers. These Lagrange multipliers, corresponding to reaction forces on the nodes where the conditions are applied, give rise to a modification of the local stresses in comparison to the surface forces applied in the finite element code. On the surfaces T_0 and T_1, no surface forces are applied, the development of stresses on these surfaces (for example circumferential stresses when an internal pressure loading

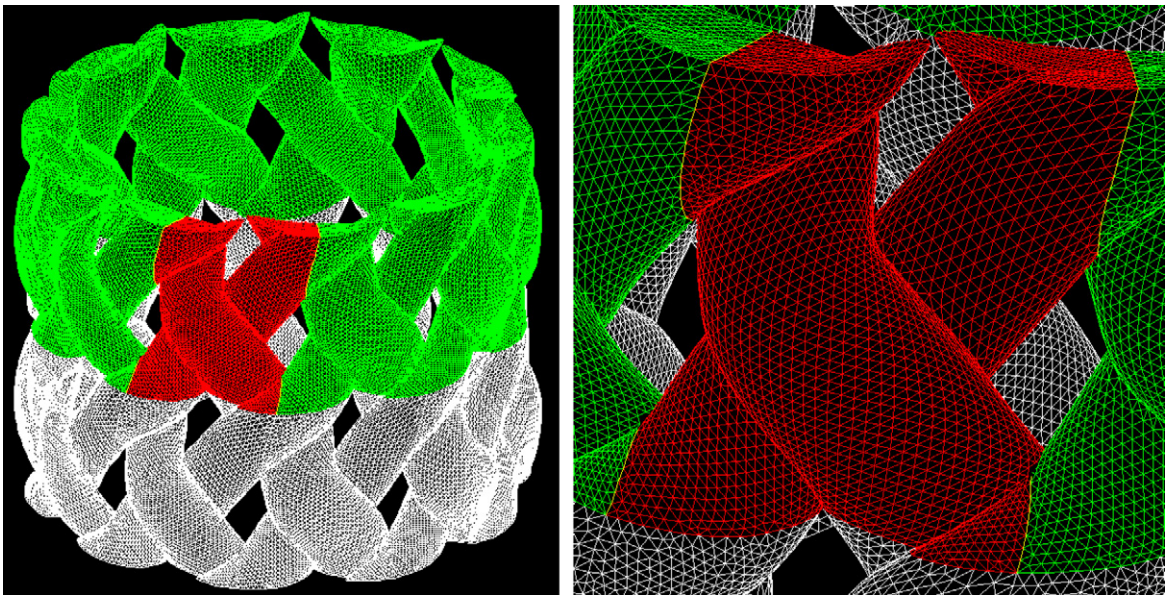

Fig. 2. Deformed unit-cell of a woven composite (in red) submitted to a combined traction–torsion loading. White and green meshes are periodic copies of the red deformed mesh.

is applied) is the consequence of the kinematic periodic boundary conditions prescribed on these surfaces (Eq. (8)). Similarly, on the surfaces Z_0 and Z_1 the applied surface forces are $-\sigma^0_{zz}\underline{e_z}$ and $\sigma^0_{zz}\underline{e_z}$ respectively, and the kinematic periodic boundary conditions (Eqs. (10) and (11)) induce additional stress fluctuations (denoted $\underline{r}$ in Eq. (3)).

It is worth mentioning that the definition of this set of boundary conditions is quite general and is not related to any underlying assumption on the considered unit-cell. As a consequence it can be applied to any heterogeneous periodic unit-cell. Fig. 2 gives the example of a woven composite submitted to a combination of traction and torsion. The simulation is performed on the red unit-cell mesh and white and green meshes are just periodic copies of the red deformed mesh. This figure validates the ability to reproduce periodicity conditions even in the case of a heterogeneous unit-cell (note that the deformation of the unit-cell is clearly heterogeneous).

4. Periodic homogenization for composite tubes with a coarse microstructure

Assuming a periodic tube defined by its periodic unit-cell, the periodic boundary conditions defined in Section 3 allow determining the exact stress strain fields for various loadings. The question is now to derive an equivalent homogeneous elastic behaviour from these results. As the stress and strain fields are heterogeneous even in the case of a homogeneous unit cell, defining effective stress and strains is quite difficult. However, two different approaches, inspired from the "mechanical" and "energetic" approaches introduced in Section 2, are proposed. These approaches converge towards the flat unit-cell approximation when the diameter of the tube is large enough whereas for lower diameters, the three approaches provide different results. As a consequence, the comparison of these results as a function of the diameter can be used (see Section 5) to evaluate the value of the diameter below which the flat unit-cell approximation is no more valid. Note that below this value, none of these approaches is really relevant. The question itself of replacing the heterogeneous media by a homogeneous equivalent media is probably not relevant and should be reviewed. This question is out of the scope of the present article.

4.1. "Mechanical approach"

Considering a homogeneous anisotropic behaviour cylindrically distributed, the stresses and strains in each point of the periodic cell are related by the stiffness tensor. When considering a Cartesian coordinate system, the expression of the stiffness tensor depends on the position of the considered point x (Eq. (12)). The superscript * stands for "expression of the tensor in the Cartesian coordinate system".

$$\underline{\underline{\sigma}}^*(x) = K^{0*}(x) : \underline{\underline{\varepsilon}}^*(x) \tag{12}$$

When considering a cylindrical coordinate system, its expression becomes independent of the position of x (Eq. (13)). The superscript ^{c} stands for "expression of the tensor in the cylindrical coordinate system".

$$\underline{\underline{\sigma}}^c(x) = K^{0c} : \underline{\underline{\varepsilon}}^c(x) \tag{13}$$

This equation can be averaged over the periodic cell (Eq. (14)), where $\overline{\underline{\underline{X^c}}}$ is a tensor defined by its components in the cylindrical coordinate system corresponding to a volume average of each components of $\underline{\underline{X^c}}$ (Eq. (15)).

$$\overline{\underline{\underline{\sigma^c}}} = K^{0c} : \overline{\underline{\underline{\varepsilon^c}}} \tag{14}$$

$$\overline{\underline{\underline{X^c}}} = \begin{pmatrix} \overline{X^c_{rr}} & \overline{X^c_{r\theta}} & \overline{X^c_{rz}} \\ \overline{X^c_{\theta r}} & \overline{X^c_{\theta\theta}} & \overline{X^c_{\theta z}} \\ \overline{X^c_{zr}} & \overline{X^c_{z\theta}} & \overline{X^c_{zz}} \end{pmatrix} \tag{15}$$

Considering a heterogeneous microstructure and similarly to the "mechanical" approach introduced in Section 2, the homogeneous equivalent tensor can be defined from Eqs. (14) and (15), using $\underline{\underline{\sigma^c}}$ and $\underline{\underline{\varepsilon^c}}$ the heterogeneous stress and strain fields, expressed in the cylindrical coordinate system. In order to determine the full tensor, 6 independent loadings are required (Eq. (14) applied for 6 independent loadings defines a 36×36 linear system where the 36 coefficients of the tensor are unknown). This definition is based on the equivalence between the heterogeneous and homogeneous cases for the quantities $\overline{\underline{\underline{\sigma^c}}}$ and $\overline{\underline{\underline{\varepsilon^c}}}$.

4.2. "Energetic approach"

The homogeneous equivalent behaviour can also be defined from an energetic point of view. The equivalent homogeneous behaviour is defined here as the homogeneous behaviour (i.e. radially distributed) for which the deformation energy function $e_{IJ}^{\hom}(K^{0c})$ is equal, for all loadings I and J, to the deformation energy e_{IJ}^{het} associated to the heterogeneous microstructure (Eq. (16)). These deformation energies are defined by Eqs. (17) and (18) from the stress and strain fields evaluated for the homogeneous behaviour ($\underline{\underline{\sigma_{0I}}}$ and $\underline{\underline{\varepsilon_{0I}}}$) and for the heterogeneous behaviour ($\underline{\underline{\sigma_{1I}}}$ and $\underline{\underline{\varepsilon_{1I}}}$), respectively. For the homogeneous behaviour, the function $e_{IJ}^{\hom}(K^{0c})$ can be expressed as a function of the stiffness (and compliance) tensors expressed in the cylindrical coordinate system (Eq. (19)).

$$e_{IJ}^{het} = e_{IJ}^{\hom}\left(K^{0c}\right) \quad \text{for } I = 1,\dots,6,\ J = 1,\dots,6 \tag{16}$$

$$e_{IJ}^{\hom}\left(K^{0c}\right) = \frac{1}{2V}\int_V \underline{\underline{\sigma_{0I}}}(x) : \underline{\underline{\varepsilon_{0J}}}(x)\,\mathrm{d}V \tag{17}$$

$$e_{IJ}^{het} = \frac{1}{2V}\int_V \underline{\underline{\sigma_{1I}}}(x) : \underline{\underline{\varepsilon_{1J}}}(x)\,\mathrm{d}V \tag{18}$$

$$e_{IJ}^{\hom}\left(K^{0c}\right) = \frac{1}{2V}\int_V \underline{\underline{\varepsilon^c_{0I}}}(x) : K^{0c} : \underline{\underline{\varepsilon^c_{0J}}}(x)\,\mathrm{d}V = \frac{1}{2V}\int_V \underline{\underline{\sigma^c_{0I}}}(x) : S^{0c} : \underline{\underline{\sigma^c_{0J}}}(x)\,\mathrm{d}V \tag{19}$$

As the stress and strain fields are heterogeneous, even for the homogeneous behaviour, the homogeneous stiffness tensor corresponding to the resolution of Eq. (16) cannot be obtained from a direct resolution of a 36×36 linear system as in the case of the periodic homogenization applied to flat unit-cells (see Eq. (3)). As a consequence, an iterative procedure has to be used. The quantities e_{IJ}^{het} for the heterogeneous unit-cell are evaluated once (from the simulations of 6 independent loadings) and the quantities $e_{IJ}^{\hom}(K^{0c})$ are evaluated for different successive values of K^{0c} in order to solve $e_{IJ}^{\hom}(K^{0c}) - e_{IJ}^{het} = 0$ (for $I = 1,\dots,6$, $J = 1,\dots,6$). In that case, K^{0c} is assumed to be symmetric and the research is performed on 21 coefficients. In practice, a Newton–Raphson algorithm can be used and each evaluation of $e_{IJ}^{\hom}(K^{0c})$ is performed numerically (i.e. finite element simulations with the same boundary conditions than those used for the heterogeneous unit-cell). Note that in order to improve efficiency, the analytical solutions evaluated for homogeneous (i.e. radially distributed) anisotropic behaviours [8] could also be used.

4.3. Comments

In Section 2, the "energetic" approach and the "mechanical" approaches are equivalent for periodic boundary conditions applied on flat unit-cells as it is demonstrated that they satisfy the Hill–Mandel condition [5]. In the "mechanical" approach proposed for the non-flat unit-cell in Section 4.1, the definition of the effective stress and strain (averaging components in the cylindrical coordinates) is quite arbitrary and the Hill–Mandel condition is not rigorously satisfied (leading to non-symmetric effective tensors as mentioned in Section 5). In the "energetic" approach (Section 4.2), the effective behaviour is defined from a purely energetic point of view without defining explicitly effective stress and strain. As a consequence, these approaches are not equivalent. However, for large enough diameters, these approaches converge together and towards the flat unit-cell approximation which satisfies the Hill–Mandel condition. Hence, considering a convergence criterion (an example is proposed in Section 5), a minimum diameter can be determined for which the equivalence between these "energetic" and "mechanical" approaches is approximately satisfied (according to the convergence criterion).

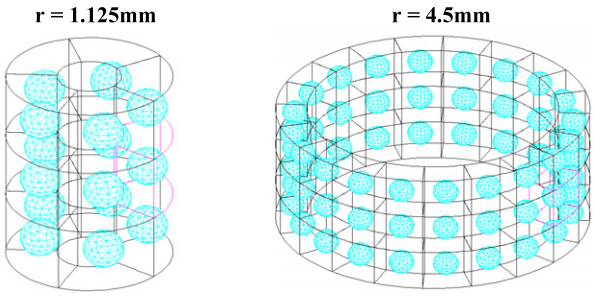

Fig. 3. Microstructures for two different mean radius of the tube (1.125 and 4.5 mm).

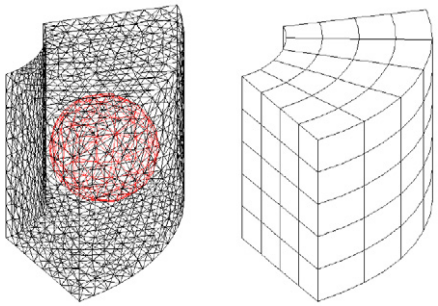

Fig. 4. Meshes used for the heterogeneous and homogeneous simulations.

5. Application to a tube with spherical inclusions

The microstructure consists of a tube with spherical inclusions periodically distributed assuming that the arc length between inclusion centres is constant as a function of the radius of the tube (Fig. 3). The "mechanical" and "energetic" approaches proposed for the non-flat unit-cells in the previous section are compared to the flat periodic unit-cell approximation (corresponding to an infinite radius) in order to discuss the validity of this approximation as a function of the tube diameter.

5.1. Description of the microstructure

The thickness of the tube is 1 mm and 4 different mean radii are considered (1.125, 2.25, 4.5 and 9 mm). The typical dimensions of the periodic inclusion network are defined by the arc length P_0 (~ 1.41 mm) between two inclusion centres and by the diameter of the inclusion d_0 (0.8 mm). In the Z direction, the distance between two inclusion centres is assumed to be equal to P_0. The number of inclusions distributed on the circumference of the tube is then 5, 10, 20 and 40 respectively for tubes of mean radii 1.125, 2.25, 4.5 and 9 mm (Fig. 3).

In order to compare results obtained for an infinite radius, a parallelepiped flat unit-cell is also considered with a thickness equal to the thickness of the tube, a width and length equal to P_0.

Finally, a high elastic contrast is assumed between the matrix and the inclusions with Young moduli of 100 GPa and 0.1 GPa respectively (Poisson coefficients are 0.3 for both the inclusions and the matrix).

The mesh refinements used for the simulations (Fig. 4) have been optimized to avoid mesh dependencies on the evaluation of the homogenized behaviours. Tetrahedral elements (10 nodes, 5 Gauss points) and cubic elements (20 nodes, 27 Gauss points) have been used respectively for the simulations on the heterogeneous and homogeneous unit-cells (required for the "energetic" approach described in Section 4.2.1).

5.2. Results

In the following, the homogenized behaviours are referenced by K^{mech} and K^{ener} respectively for the "mechanical" approach (Eq. (14)) and the "energetic" approach (Eq. (16)). K^{∞} corresponds to the homogenized behaviour evaluated on a parallelepiped unit cell with classical periodic boundary conditions applied between surfaces T_0 and T_1, and Z_0 and Z_1, and static uniform boundary conditions on surfaces R_0 and R_1.

All the tensors evaluated numerically exhibit an orthotropic symmetry (coefficients less than 1 MPa are set to "0"). While K^{ener} is symmetric by definition, the numerical evaluation of K^{mech} exhibits a slight non-symmetry which decreases when the tube diameter increases (less than 0.3% in the worst case of the smallest radius). The numerical values presented in the following are symmetrized values (for non-diagonal coefficients $K_{ij}^{mech} \approx 1/2(K_{ij}^{mech} + K_{ji}^{mech})$).

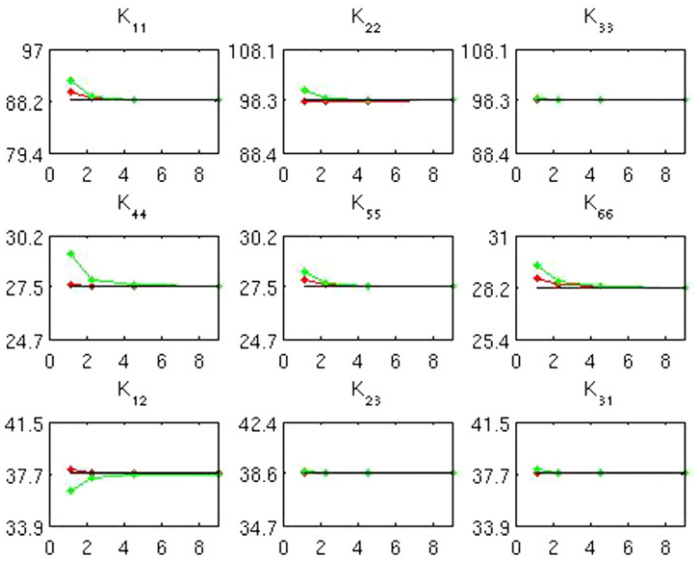

Fig. 5. Evolution of the non-zero coefficients of the homogenized stiffness tensors as a function of the mean radius of the tube (Y-axis in GPa, X-axis in mm). K^{mech}, K^{ener} and K^{∞} are respectively plotted in red, green and black. The scale of the Y-axis is defined for each coefficient by $[0.9K_{IJ}^{\infty}; 1.1K_{IJ}^{\infty}]$. Coefficients are expressed with the Voigt notation with the correspondence $1 \rightarrow rr$, $2 \rightarrow \theta\theta$, $3 \rightarrow zz$, $4 \rightarrow r\theta$, $5 \rightarrow rz$, $6 \rightarrow \theta z$.

The evolution of the coefficients are plotted as a function of the mean radius of the tube in Fig. 5 for the homogenized stiffness tensors K^{mech} and K^{ener}. It can be observed that all these tensors converge towards K^{∞} which is a satisfying result as K^{∞} corresponds to the case of the infinite radius. This point can be regarded as a partial validation of the periodic boundary conditions proposed and implemented for the non-flat unit-cells. Considering K^{mech} and K^{ener}, the convergence is achieved for a quite small radius. For a convergence criterion, defined by $\max|(K_{IJ} - K_{IJ}^{\infty})/K_{IJ}^{\infty}|$, of 2%, the results demonstrate that convergence is achieved for radii of 1.125 mm and 2.5 mm respectively for K^{mech} and K^{ener}. As a consequence, for a radius larger than 2.5 mm, convergence is achieved, the two approaches are equivalent and correspond to the evaluation of K^{∞} performed on a flat unit-cell. As a conclusion for this specific microstructure and according to the proposed convergence criterion, the flat unit-cell approximation is valid for diameters larger than 2.5 mm.

6. Conclusions and future prospects

Composite tubes with a coarse microstructure (i.e. the typical size of the microstructure is not small compared to the dimensions of the tube) are of interest for different applications such as fuel cladding tubes for nuclear application [9] or catheter for medical application [3]. In order to evaluate the stress-strain fields within the composite, finite element simulations are commonly performed on representative unit-cells. For flat composites, periodic boundary conditions are well established and widely used. In order to account for the radius of the tube in FE simulations the first question was then to extend periodic boundary conditions to non-flat unit-cells (Section 3). Then, the second question was to discuss the validity of a flat unit-cell approximation, neglecting the radius of the tube, used to evaluate a homogenized behaviour for the tube. For this discussion, two different homogenization procedures based on simulations performed with these new boundary conditions have been proposed in Section 4. They are inspired from the “mechanical” and “energetic” approaches introduced in Section 2 for flat unit-cells. These approaches converge towards the flat unit-cell approximation when increasing the diameter of the tube and a convergence criterion is proposed (Section 5) to evaluate the diameter above which the three approaches are equivalent. Below this value, the three approaches provide three different results but none of them is more relevant than another and the question itself of replacing the heterogeneous media by a homogeneous media has probably to be reviewed. It can also be noticed that the effective behaviour evaluated with the “mechanical” approach exhibits a slight non-symmetry, however, this asymmetry also decreases when the diameter increases and, for the microstructure considered in Section 5, this asymmetry is negligible especially when considering diameters satisfying the convergence criterion.

Finally, the conclusion given is Section 5 is specific of the considered microstructure and a further work will be to account for more realistic microstructures. In addition, the second part of the present paper was focused on the overall elastic behaviour and average quantities; it will be of a great interest to compare the effect of the radius of the tube on the local stresses and strains especially when considering non-linear behaviours.

References

[1] G. Chatzigeorgiou, N. Charalambakis, F. Murat, Homogenization problems of a hollow cylinder made of elastic materials with discontinuous properties, International Journal of Solids and Structures 45 (18–19) (2008) 5165–5180.

[2] G. Chatzigeorgiou, N. Charalambakis, F. Murat, Homogenization of a pressurized tube made of elastoplastic materials with discontinuous properties, International Journal of Solids and Structures 46 (21) (2009) 3902–3913.
[3] C. Ayranci, J.P. Carey, Predicting the longitudinal elastic modulus of braided tubular composites using a curved unit-cell geometry, Composites Part B: Engineering 41 (3) (2010) 229–235.
[4] Y. Zhang, Z. Xia, F. Ellyin, Two-scale analysis of a filament-wound cylindrical structure and application of periodic boundary conditions, International Journal of Solids and Structures 45 (20) (2008) 5322–5336.
[5] M. Bornert, T. Bretheau, P. Gilormini, Homogeneisation en mécanique des matériaux, Hermes, 2001.
[6] C. Huet, Application of variational concepts to size effects in elastic heterogeneous bodies, Journal of the Mechanics and Physics of Solids 38 (6) (1990) 813–841.
[7] L. Gelebart, C. Colin, Effects of porosity on the elastic behaviour of cvi sic/sic composites, Journal of Nuclear Materials 386 (2009) 82–85.
[8] T.Y. Chen, C.T. Chung, W.L. Lin, A revisit of a cylindrically anisotropic tube subjected to pressuring, shearing, torsion, extension and a uniform temperature change, International Journal of Solids and Structures 37 (37) (2000) 5143–5159.
[9] P. Yvon, F. Carré, Structural materials challenges for advanced reactor systems, Journal of Nuclear Materials 385 (2) (2009) 217–222.